MULTI-POINT LEAST SQUARES MATCHING WITH ARRAY RELAXATION UNDER VARIABLE WEIGHT MODELS

Xiaoliang Wu

Space Centre for Satellite Navigation, Queensland University of Technology
GPO Box 2434 QLD 4001, Australia   E-mail: wux@redash.qut.edu.au

KEY WORDS: Three-dimensional Reconstruction, Global Image Matching, Array Algebra, Relaxation, Lest Squares Matching

ABSTRACT

In this paper, An algorithm called Array Relaxation Multi-point Least Squares Matching (ARMLSM) will be discussed in detail, and the new formulation of Array Relaxation under the variable constraint weight model is presented. The presented new ARMLSM can take into account both cases of the first and second order derivative constraint weight models, and the new ARMLSM can be applied in the both of image space and object space. A hierarchical strategy is used in the ARMLSM in order to derive the matching approximations. The hierarchical ARMLSM approach limits the searching range for matching candidates in each image pyramid level and therefore can also improve computing efficiency.

Three test image pairs are used. The matching results of the conventional MLSM, the ARMLSM under the optimal uniform constraint weight model and the ARMLSM under the variable constraint weight model are compared and analysed. Three matching efficiencies are found to be near 6, 82 and 81 node points per second on *SGI 4D/25*, respectively, and the matching accuracy comparison of the Loess plateau aerial images shows 0.79, 0.75 and 0.37 pixels can be reached by the three MLSM algorithms, respectively. The ARMLSM under the variable constraint weight model has great potential for practical digital photogrammetric systems.

1 INTRODUCTION

During the last few decades a vast variety of image matching methods have been developed, most of them belong to single point or features/edge matching algorithms, Reconstructing three-dimensional (3-D) surfaces is an ill-posed problem from the mathematical point of view, recently more and more Global Image Matching (GIM) techniques have been used in 3-D reconstruction applications such as regularization theory [8, 18], stochastic optimal approach using microcanonical annealing [2, 3], neural network stereo matching [21] etc.. Various kinds of assumptions and constraints were introduced in these GIM methods in order to get more reliable and acceptable solutions than the single point or single feature/edge matching.

Multi-point Least Squares Matching (MLSM) is one of GIM techniques which was developed from the single point Least Squares Matching (LSM) by many researchers: Rosenholm [16, 17], Rauhala [10, 13] and Li [6, 7] etc.. Compared to other GIM techniques, MLSM is widely used in the photogrammetric community, MLSM uses simultaneous computation of parallaxes in the grid which are connected with bilinear finite elements describing the parallaxes differences. It is assumed that the object model is a continuous surface, the additional fictitious observations for continuity constraints on parallaxes are used in MLSM. MLSM is not only applied in the image space but also in object space [4, 5, 16, 20].

GIM (including MLSM) can provide much more reliable and accurate matching results than the single point matching method, for example, MLSM based on image space can reach 0.1 ~ 0.5 pixel accuracy [15] and MLSM based on object space can reach 0.15 ~ 0.2 pixel [16], 0.25 pixel [19]. However, no matter what kind of GIM method is used, the low computational efficiency is the common shortcoming. How to improve the computational efficiency is the problem faced in all GIM methods, Li [6] uses MLSM in a multiresolution, multigrid approach, the average CPU time improvement was 60% (corresponding to 6 points per second based on our test).

It is desirable for MLSM that the constraint weights should be small enough if the object surface and image intensity changes are severe such as for the ridges, breaklines and valleys, on the other hand, the constraint weights should be big enough if the surface and intensity changes are gentle such as for flat open areas. In this paper the proposed new ARMLSM (Array Relaxation MLSM) which was developed from Rauhala's Global Least Squares Matching (GLSM) ideas is a good example of such MLSM, it rightly takes into account the object surface details and the image intensity changes through the variable constraint weight model. ARMLSM's matching efficiency can reach about 15 times faster than the conventional MLSM's.

In the following, the first two sections give a brief description of the conventional MLSM and Rauhala's optimal weight model ARMLSM, then the new ARMLSM under the variable weight model will be presented, in Section 5, we combine multiresolution strategy and the new ARMLSM into our Hierarchical ARMLSM, and finally, tests and conclusions are discussed.

2 CONVENTIONAL MLSM

Assuming the parallax of a left epipolar line point $g_1(x, y)$ is $-x^0$, the observation of the single least squares matching is (ignoring the radiometric deformation):

$$g_1(x, y) - g_2(x + x^0, y) = n(x, y) \qquad (1)$$

where $g_2(x + x^0, y)$ is the corresponding point of $g_1(x, y)$ in right epipolar line, and $n(x, y)$ means the random noise.

If the x-parallax is interpolated from its four neighbour grid nodes through bilinear interpolation, the spacing between neighbour nodes is 1 and the distances from the point to node (i, j) are d_1 and d_2 ($0 \le d_1, d_2 \le 1$), then the error

977

International Archives of Photogrammetry and Remote Sensing. Vol. XXXI, Part B3. Vienna 1996

equation is:

$$v = g_2'(1-d_1)(1-d_2)dx_{i,j} + g_2'd_1(1-d_2)dx_{i,j+1} + \\ g_2'(1-d_1)d_2dx_{i+1,j} + g_2'd_1d_2dx_{i+1,j+1} - \Delta g \tag{2}$$

where $\Delta g = g_1(x,y) - g_2(x+x^0,y)$ and g_2' is the differential in x-direction in right epipolar line and dx_{ij} is the correction of original parallax x^0.

Assuming all the matching points are located on a grid sized by $n_1 \times n_2$ (n_1 is rows and n_2 is columns). The constraint smoothness between the grid nodes is required in MLSM (first or second order differentials of parallaxes). The observations, normals and solution of MLSM can be expressed in the matrix form:

$$V = AdX - L, P \\ (A^TPA)dX = A^TPL \\ dX = (A^TPA)^{-1}A^TPL \tag{3}$$

where A is the design matrix, dX is the vector of correction parallaxes ($n_1n_2 \times 1$) and P is the weight matrix.

Likewise MLSM can be performed in object space using the similar equations as in image space [4, 5, 20].

The main reason for the very low computing efficiency of the conventional MLSM is the solution of the large size normals. For example, the rank of the normals is 10,000 if the matching grid is 100 by 100, it is hard to be solved for the general purpose computer. Some techniques are used for improving the speed of the conventional MLSM such as multiresolution, multigrid approach [6], the average CPU time improvement was 60%, corresponding 2 3 node points per second. Besides it, the Cholesky triangle decomposition technique is used, and the speed of image matching is about 6 node points per second (platform *SGI 4D/25*). In the next sections we will discuss the array relaxation algorithm which can be applied for MLSM to considerably improve the matching efficiency.

3 ARMLSM UNDER THE UNIFORM WEIGHT MODEL

3.1 Introduction of array algebra

Array Algebra was established by Rauhala in 1968, and it has become the powerful tools to deal with multi-dimensional data since 1968. The basic theory of array algebra could be found in [9]. The application of array algebra in image matching can be traced back to 1977 [10], when Rauhala combined the array algebra with finite element method, and applied the array relaxation technique in global image correlation. This thought is actually different in approach but equally satisfactory in result combining with Helava, Wrobel, Rosenholm, Ebner, Heipke and Barnard's algorithms of global image matching. And the capability of array relaxation makes Rauhala's method more practicable.

3.2 ARMLSM under the uniform weight model

Assuming x^0 in equation 1 is the node point parallax and need not be interpolated from other node points. The linearised form of equation 1 is as follows:

$$v = g_2'dx - \Delta g \quad \Delta g = g_1 - g_2 \tag{4}$$

The expression of the correction of x^0 parallax after normalling equation 4:

$$dx = \sum g_2' \Delta g / \sum g_2'^2 \tag{5}$$

Equation 5 is the simplest case of the single point LSM, where $\sum$ means the sum in a small window around the node point. If the matching grid is $n_1 \times n_2$, then three matrices dX, A, L denote the three array of all node points' parallaxes corrections, grey differentials and reflection differences, respectively:

$$dX = \begin{bmatrix} dX_{11} & dX_{12} & \cdots & dX_{1n_2} \\ dX_{21} & dX_{22} & \cdots & dX_{2n_2} \\ \vdots & \vdots & \cdots & \vdots \\ dX_{n_11} & dX_{n_12} & \cdots & dX_{n_1n_2} \end{bmatrix}$$

$$A = \begin{bmatrix} g_{211}' & g_{212}' & \cdots & g_{21n_2}' \\ g_{221}' & g_{222}' & \cdots & g_{22n_2}' \\ \vdots & \vdots & \cdots & \vdots \\ g_{2n_11}' & g_{2n_12}' & \cdots & g_{2n_1n_2}' \end{bmatrix} \tag{6}$$

$$L = \begin{bmatrix} \Delta g_{11} & \Delta g_{12} & \cdots & \Delta g_{1n_2} \\ \Delta g_{21} & \Delta g_{22} & \cdots & \Delta g_{2n_2} \\ \vdots & \vdots & \cdots & \vdots \\ \Delta g_{n_11} & \Delta g_{n_12} & \cdots & \Delta g_{n_1n_2} \end{bmatrix}$$

and the array expression of MLSM is:

$$V = A * dX - L \tag{7}$$

where $*$ means elementwise array multiplication.

In equation 7 the relationship between node points has not been considered yet, so fictitious equations are also needed here. Assuming x is the true parallaxes, its initial value is x^0, the correction is dx. Firstly the second order differential constraint is considered:

$$x_{i+1,j} - 2x_{i,j} + x_{i+1,j} = 0 \\ x_{i,j-1} - 2x_{i,j} + x_{i,j+1} = 0 \tag{8}$$

The array expression of equation 12 is:

$$V_y = (2I_1 + B)(X^0 + dX), p_1 \\ V_x = (X^0 + dX)(2I_2 + B_2), p_2 \tag{9}$$

where the matrix ranks of subscript 1 and 2 are n_1 and n_2, respectively. I is an unit matrix, B is a Toeplitz matrix, and p_1, p_2 are the weights in y, x directions.

$$B = \begin{bmatrix} 0 & -1 & & & & \\ -1 & 0 & -1 & & & \\ & -1 & 0 & -1 & & \\ & & \ddots & \ddots & \ddots & \\ & & & & & -1 \\ & & & & -1 & 0 \end{bmatrix}$$

$$B = S^T\lambda S, S^TS = SS^T = I$$
$$S = \{s_{ij}\} = (-1)^i \sin(ij\pi/(n+1))\sqrt{(n+1)/2}$$
$$\lambda = \{\lambda_{ii}\} = -2\cos(i\pi/(n+1)), i,j = 1,2,\cdots,n \tag{10}$$

The Toeplitz matrix B's feature and orthogonal matrix can be derived through the finite element transformation [11] (see equation 10), and an approximation is applied near the edges of the net grid inside the matrix B.

The array expression of ARMLSM under the second order differential constraint is:

$$V = A * dX - L \\ V_y = (2I_1 + B_1)(X^0 + dX), p_1 \\ V_y = (X^0 + dX)(2I_2 + B_2), p_2 \tag{11}$$

978

International Archives of Photogrammetry and Remote Sensing. Vol. XXXI, Part B3. Vienna 1996

In the same way, the array expression of ARMLSM under the first order differential constraint is:

$$V = A * dX - L$$
$$V_y = C_1(X^0 + dX), p_1$$
$$V_y = (X^0 + dX)C_2, p_2$$

(12)

where

$$C_1 = \begin{bmatrix} 1 & -1 & & & \\ & 1 & & & \\ & & \ddots & -1 & \\ & & & 1 \end{bmatrix} \quad C_2 = \begin{bmatrix} 1 & & & \\ -1 & 1 & & \\ & & \ddots & \\ & & -1 & 1 \end{bmatrix}$$

(13)

when n_1, n_2 are large enough, $C_1^T C_1 \approx 2I_1 + B_1, C_2^T C_2 \approx 2I_2 + B_2$. The normals of equations 11 or 12 are:

$$E * dX + p_1 S_1^T (2I_1 + \lambda_1)^k S_1 dX + dX S_2^T (2I_2 + \lambda_2)^k S_2 p_2$$
$$= U_1 - p_1 S_1^T (2I_1 + \lambda_1)^k S_1 X^0 - X^0 S_2^T (2I_2 + \lambda_2)^k S_2 p_2$$
$$E = \{e_{ij}\} = \{\sum (g_2')_{ij}^2\} \quad U_1 = \{u_{ij}\} = \{\sum (g_2' \Delta g)_{ij}\}$$

(14)

where $k = 1$ or $k = 2$ means the first or second order differential constraint case.

Because the normals of ARMLSM is different from conventional normals (see equation 3), in the following section, the array relaxation solution will be introduced.

ARMLSM solution under the uniform weight model Assuming:

$$E = \bar{e} + E - \bar{e} \quad \bar{e} = \sum \sum e_{ij}/(n_1 n_2)$$

(15)

putting equation 15 into equation 14 and moving $(e - \bar{e}) * dX_0$ into the right hand side where dX_0 is the last corrections:

$$\bar{e} dX + p_1 S_1^T (2I_1 + \lambda_1)^k S_1 dX + dX S_2^T (2I_2 + \lambda_2)^k S_2 p_2$$
$$= U_1 - p_1 S_1^T (2I_1 + \lambda_1)^k S_1 X^0 - X^0 S_2^T (2I_2 + \lambda_2)^k S_2 p_2$$
$$-(E - \bar{e}) * dX_0$$

(16)

the normals are diagonallized by premultiplication with S_1 and postmultiplication with S_2^T, and considering $S^T S = I$,

we derived:

$$D * (S_1 dX S_2^T = S_1 U_k S_2^T =$$
$$S_1 U_1 S_2^T - G * (S_1 X^0 S_2^T) - S_1[(E - \bar{e}) * dX_0]S_2^T$$

(17)

where

$$g_{ij} = p_1(2 + (\lambda_1)_{ii})^k + p_2(2 + (\lambda_2)_{jj})^k$$
$$d_{ij} = \bar{e} + g_{ij}$$

(18)

Assuming $h_{ij} = 1/d_{ij}$:

$$dX_{k+1} = S_1^T(H * S_1 U_k S_2^T)S_2$$

(19)

Equation 19 is the iterative formula of the uniform weight ARMSLM.

4 NEW ARMLSM

It will be very desirable that the weight model inside ARMLSM can be adjustable under a various types of terrain: the weight constraint should be relaxed if ridges, valleys, breaklines etc. are met, the weight constraint condition should be strengthened if in the flat areas. To solve these problems Rauhala et al [14] used 15 math models of the continuity constraints to improve the continuity strength effected by g_{ij} in equation 22. However, all these models can only enhance or relax the continuity strength globally due to the fact that p_1 and p_2 are two constants for all grid points. The ARMLSM algorithm described by [12] is called the optimal uniform weight model ARMLSM here. We think it has not provided the capabilities to allow each different weight to appear in each grid point in order to adjust the continuity constraint according to the local terrain and intensity details. To able to do this, a new ARMLSM is presented here which is called the variable weight model ARMLSM.

4.1 ARMLSM under the variable weight model

When the xy–direction weights are two arrays P_1 and P_2 instead of two weight constants p_1 and p_2 in equation 14, in order to derive the new normals, two new arrays N_y and N_x are defined:

if $k = 2$:

$$N_y = \begin{bmatrix} 4p_{1j} + p_{2j} & -2p_{1j} - 2p_{2j} & p_{2j} & & & \\ -2p_{1j} - 2p_{2j} & p_{1j} + 4p_{2j} + p_{3j} & -2p_{2j} - 2p_{3j} & p_{3j} & & \\ p_{2j} & -2p_{2j} - 2p_{3j} & p_{2j} + 4p_{3j} + p_{4j} & -2p_{3j} - 2p_{4j} & p_{4j} & \\ & & \ddots & \ddots & \ddots & \ddots \\ & & & p_{n_1-1,j} & -2p_{n_1-1,j} - 2p_{n_1,j} & p_{n_1-1,j} + 4p_{n_1,j} \end{bmatrix}$$

$$N_x = \begin{bmatrix} 4p_{i1} + p_{i2} & -2p_{i1} - 2p_{i2} & p_{i2} & & & \\ -2p_{i1} - 2p_{i2} & p_{i1} + 4p_{i2} + p_{i3} & -2p_{i2} - 2p_{i3} & p_{i3} & & \\ p_{i2} & -2p_{i2} - 2p_{i3} & p_{i2} + 4p_{i3} + p_{i4} & -2p_{i3} - 2p_{i4} & p_{i4} & \\ & & \ddots & \ddots & \ddots & \ddots \\ & & & p_{i,n_2-1} & -2p_{i,n_2-1} - 2p_{i,n_2} & p_{i,n_2-1} + 4p_{i,n_2} \end{bmatrix}$$

(20)

if $k = 1$:

$$N_y = \begin{bmatrix} p_{1j} & -p_{1j} & & \\ -p_{1j} & p_{1j} + p_{2j} & -p_{2j} & \\ & \ddots & \ddots & \ddots \\ & & -p_{n_1-1,j} & p_{n_1-1,j} + p_{n_1,j} \end{bmatrix} \quad N_x = \begin{bmatrix} p_{i1} & -p_{i1} & & \\ -p_{i1} & p_{i1} + p_{i2} & -p_{i2} & \\ & \ddots & \ddots & \ddots \\ & & -p_{i,n_2-1} & p_{i,n_2-1} + p_{i,n_2} \end{bmatrix}$$

(21)

where $j = 1, \cdots, n_2$ and $i = 1, \cdots, n_1$.

N_y and N_x are not usual matrices because the elements p_{ij} are dynamically changed during the special definition of two

979

International Archives of Photogrammetry and Remote Sensing. Vol. XXXI, Part B3. Vienna 1996

matrices multiplication in our new ARMLSM. A new multiplication symbol is defined in our new ARMLSM: $\odot$, $N_y \odot X$ means the multiplication of two matrices N_y and X where the subscript j in array N_y is changed according to the current corresponding column number in matrix X, and $X \odot N_x$ has the same meaning where subscript i in array N_x is changed according to the current corresponding row number in matrix X. And the new normals are:

$$E * dX + N_y \odot dX + dX \odot N_x = U_1 - N_y \odot X^0 - X^0 \odot N_x \tag{22}$$

where E and U_1 are the same as in equation 14.

4.2 ARMLSM solution under the variable weight model

Assuming:

$$\begin{aligned} E &= \bar{e} + E - \bar{e} & \bar{e} &= \sum\sum e_{ij}/(n_1 n_2) \\ N_y &= \overline{P_1} + N_y - \overline{P_1} & \overline{p_1} &= \sum\sum p_{1ij}/(n_1 n_2) \\ N_x &= \overline{P_2} + N_x - \overline{P_2} & \overline{p_2} &= \sum\sum p_{2ij}/(n_1 n_2) \end{aligned} \tag{23}$$

putting equation 23 into equation 22 and moving $(e - \bar{e}) * dX_0$, $((N_y - \overline{P_1}) \odot dX_0$ and $dX_0 \odot (N_x - \overline{P_2})$ into the right hand side where dX_0 is the last time corrections, we derived:

$$\begin{aligned} \bar{e} dX + \overline{p_1} S_1^T (2I_1 + \lambda_1)^k S_1 dX + dX S_2^T (2I_2 + \lambda_2)^k S_2 \overline{p_2} &= \\ U_1 - N_y \odot X^0 - X^0 \odot N_x - (E - \bar{e}) * dX^0 & \\ -(N_y - \overline{P_1}) \odot dX^0 - dX^0 \odot (N_x - \overline{P_2}) & \end{aligned} \tag{24}$$

The N_y and N_x are based on the elements values in equations 20 or 21. The normals are diagonallized by premultiplication with X_1 and postmultiplication with S_2^T, and considering $S^T S = I$, we derived:

$$\begin{aligned} D * (S_1 dX S_2^T &= S_1 U_k S_2^T = \\ S_1 U_1 S_2^T - G * (S_1 X^0 S_2^T) - S_1[(E - \bar{e}) * dX_0] S_2^T \end{aligned} \tag{25}$$

where

$$\begin{aligned} g_{ij} &= p_1 (2 + (\lambda_1)_{ii})^k + p_2 (2 + (\lambda_2)_{jj})^k \\ d_{ij} &= \bar{e} + g_{ij} \end{aligned} \tag{26}$$

Assuming $h_{ij} = 1/d_{ij}$:

$$dX_{k+1} = S_1^T (H * S_1 U_k S_2^T) S_2 \tag{27}$$

Equation 27 the iterative formula of the variable weight model ARMSLM. Due to $S_1 U_{k+1} S_2^T = H * S_1 U_k S_2^T$, so $H * S_1 U_k S_2^T$ can be used as $S_1 dX^0 S_2^T$ for the next iteration computation, need not be computed again.

When the values of all elements in P_1 or P_2 are equal (say equal to p_1 or p_2, respectively), equation 24 becomes equation 16. It means the uniform weight model ARMLSM is the special case of the variable weight model ARMLSM.

4.3 Object space based ARMLSM

If the ARMLSM is performed in object space, the matching grid will be based on the object space coordinate system instead of the parallaxes grid in image space. Assuming only one stereo image pair is used, object space based ARMLSM has all the similar formulas except the parallaxes array X^0 and dX need to be replaced by the elevation array Z^0 and dZ, and the E and U_1 are changed into:

$$\begin{aligned} E &= \{e_{ij}\} = \{\sum (g')_{ij}^2\} \\ U_1 &= \{u_{ij}\} = \{\sum (g_2' \Delta g)_{ij}\} \\ g' &= \frac{\partial g_2}{\partial x}\frac{\partial x}{\partial Z} + \frac{\partial g_2}{\partial y}\frac{\partial y}{\partial Z} - \frac{\partial g_1}{\partial x}\frac{\partial x}{\partial Z} - \frac{\partial g_1}{\partial y}\frac{\partial y}{\partial Z} \\ \Delta g &= g_1^0(x_1, y_1) - g_2^0(x_2, y_2) \end{aligned} \tag{28}$$

4.4 Weight models

The weight model plays an important role in the new ARMLSM. Ideally the weight model should reflect the affection both of the terrain feature and image intensity functions, but the two functions are often inconsistent, it results in the difficulties of choice of the weight model. The main factor which effects the single point LSM is the image texture information [1], so currently our weight model is only relative with the image intensity. The variance, differential, gradient, entropy can be considered to determine the weights. The following is our method of selecting weights:

1. computing the mean differentials $(\overline{g_x}, \overline{g_y})$ of differentials g_{xij} and g_{yij} in the matching window around the grid node

2. finding $\min \overline{g_x}$, $\min \overline{g_y}$, $\max \overline{g_x}$ and $\max \overline{g_y}$

3. determining the weights p_{xij} and p_{yij} for each grid node point:

$$\begin{aligned} p_{yij} &= C_2 + (\max \overline{g_x} - h_{xij}) \frac{p_1}{\max \overline{g_x} - \min \overline{g_x}} \\ p_{xij} &= C_1 + (\max \overline{g_y} - h_{yij}) \frac{p_2}{\max \overline{g_y} - \min \overline{g_y}} \end{aligned} \tag{29}$$

where p_1, p_2, C_1, C_2 are experiential constants, we recommend $p_1 = p_2 = 100$ and $C_1 = C_2 = 10$, they are adjustable based on the image texture and terrain undulation

4.5 New ARMLSM's computation efficiency

Assuming the matching grid size is $n \times n$, generally the traditional MLSM needs about $(n)^6$ multiplication operations. According to our new ARMLSM, the multiplication operations in each iteration are $8n^3$ (actually are $8n^3 + 3n^2$, while $S_1 dX_0 S_2^T$ need not be calculated since the second iteration, so we simplify to $8n^3$ for convenience), again assuming the total iteration is k, the operations count ratio between our ARMLSM and the traditional MLSM is:

$$Ratio = 8k/n^3 \tag{30}$$

our experiments show that k usually takes 3 or 4 iterations.

5 PROCEDURE OF ARMLSM

We mentioned previously the new ARMLSM can be applied in both image space and object space, and employs a hierarchical strategy, here are the algorithm procedures:

Image space based ARMLSM

1. generating the image pyramids both for left and right images, assuming total levels is K, let $k = K$

2. resampling the right image using the approximate parallaxes ($X^0 = 0$ when $k = K$)

3. performing the radiometric correction

4. array relaxing l times based on equations 25 to 27

5. correcting prime X^0, if the corrections are less a given limit, goto step 2, otherwise stop at level k

6. transferring the results from level k to level $k - 1$, let $k = k - 1$

7. if $k = 0$, finishing all levels' matching, otherwise goto step 2

980

International Archives of Photogrammetry and Remote Sensing. Vol. XXXI, Part B3. Vienna 1996
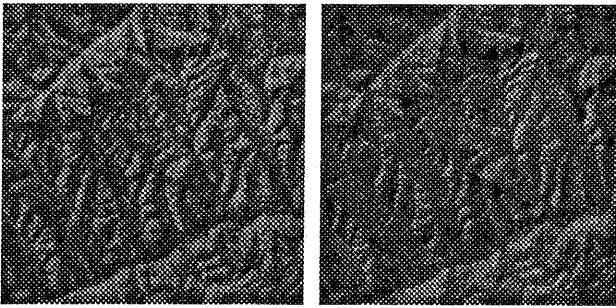
Figure 1: Loess plateau stereo images (500×500 pixels)

Object space based ARMLSM The object space based procedure for ARMLSM is exactly the same as that based on image space except for replacing X (parallaxes) by Z (heights) in all equations.

6 ARMLSM TESTING RESULTS

Three test image pairs are used: "Loess plateau" aerial images (see figure 1), "SPOT" images and ISPRS test image pair "Wall". We are only able to present "Loess plateau" results here owing to the limitation of space. Three MLSM algorithms are tested: the conventional MLSM algorithm (see section 2), ARMLSM under the optimal uniform weight model (section 3) and ARMLSM under the variable weight model (see section 4), they are abbreviated by MLSM1, MLSM2 and MLSM3 herein. The Cholesky triangle decomposition technique and hierarchy technique are used for improving the speed of the conventional MLSM solution. The object space based MLSM is only tested using SPOT images.

The computing speeds of three MLSM can be found in the table 1.

In order to check the matching accuracy, all the grid points' parallaxes of the three stereo image pairs are manually measured carefully in the workstation (for example, 5329 (73×73) points in "Loess plateau"), DEM points are also measured for "SPOT" through "VLL" method). These results are treated as the "true" parallaxes in order to compare with the automated matching results. the matching accuracy of three MLSM can be seen from the table 2. In table 2 object space based (AR)MLSM for SPOT images shows that 0.486, 0.208 and 0.187 pixels accuracy (corresponding to 12.2, 5.2 and 4.7 meters in heights) can be reached using MLSM1, MLSM2 and MLSM3, respectively.

The "Loess plateau" matching residual errors of three algorithms compared with their true parallaxes can be viewed in figures 2 where grey scale values indicate the residual levels (black colour means worst, white colour means very good matching).

The grid spacing in the above tests is 6×6 pixels (SPOT's grid intervals are 13×13). Theoretically any spacing can be used. We use 2×2 spacing for "Loess plateau" whose image size is 500×500, a very dense matching grid shown in figure 3 illustrates a much detailed terrain (233×217=50,561 points), figure 4 is its perspective view. In other words, some difficult matching areas like ridges, valleys and breaklines can be improved very much using dense ARMLSM.
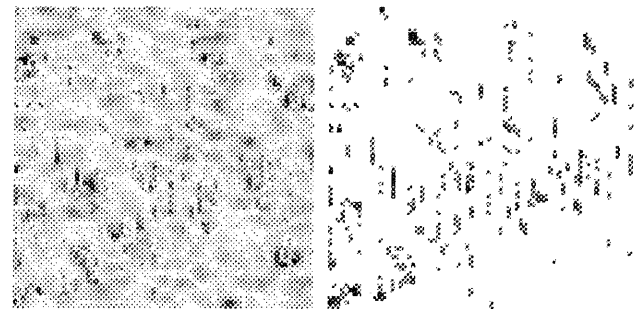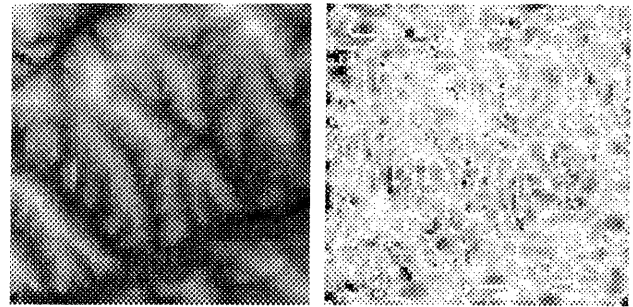

Figure 2: Loess plateau matching residual errors: left upper: true parallaxes; right upper: MLSM1 residuals; left bottom: MLSM2 residuals; right bottom: MLSM3 residuals

image & grid size	MLSM1	MLSM2	MLSM3
Plateau(73×73)	6	82	81
Wall(39×35)	18	91	85
SPOT(73×73)	6	81	78
SPOT(30×30)*	7	20	20

Table 1: matching speeds of three MLSM (unit: node points per second), (note.: * means using the object space based MLSM)

mean error	MLSM1	MLSM2	MLSM3
Plateau	0.789	0.751	0.366
Wall	1.742	1.392	0.883
SPOT	0.468	0.239	0.205
SPOT*	0.486	0.208	0.187

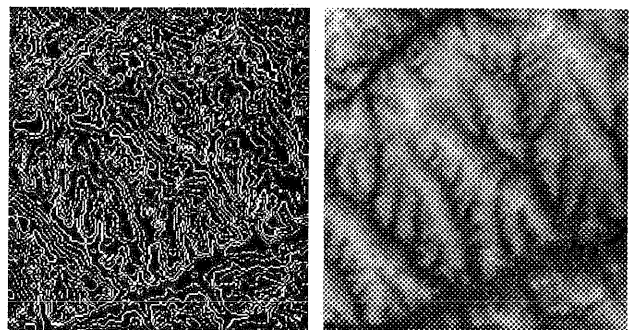Table 2: matching accuracy of three MLSM (unit: pixel), (note.: * means using the object space based MLSM)

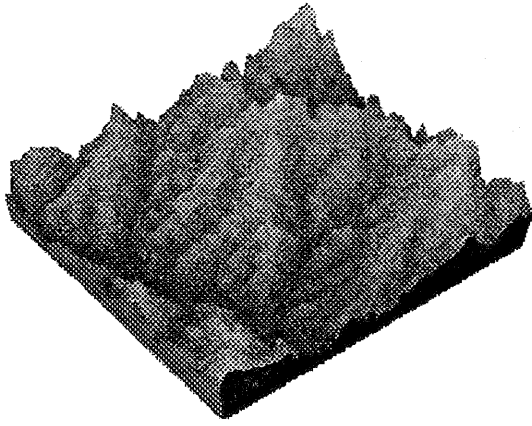Figure 3: Loess plateau's parallaxes and its grey scale image

981

International Archives of Photogrammetry and Remote Sensing. Vol. XXXI, Part B3. Vienna 1996

Figure 4: Perspective view of Loess plateau's parallaxes

7 CONCLUSIONS

Array Relaxation for Multiple-point Least Squares Matching (ARMLSM) has the great potential in the practical photogrammetric systems due to its very high computational efficiency comparing with the traditional MLSM. The new formulation of ARMLSM under the variable weight model presented by this paper makes it possible to capture the more detailed terrains through the variable weight models which are adjustable and followed the expected rule: giving tighter constraint weights in flat open areas or poor image intensity areas and looser constraint weights in rapid changed or rich information areas. The preliminary experimental results prove its ability to produce high-efficiency and high-quality image matching on the general purpose computer, and the results also show that very dense elevation models computed by our ARMLSM provide the subtle terrain details. Since the variable constraint weights can be applied in our ARMLSM, it opens a new way for using efficient array algebra technique to consider the breaklines, occlusions and discontinuity problems during the matching processing. The strategy of choosing the constraint weight discussed here is a very simple way, to find a better solution for constraint weight models becomes our current focus for the further developing of our ARMLSM.

8 ACKNOWLEDGEMENTS

I would like thank my colleague Maurice Friend for his reviews of this paper.

REFERENCES

[1] F. Ackermann, "Digital image correaltion: Performance and potential application in photogrammetry," *Photogrammetric Record*, 1984.

[2] H. H. Baker, "Multiple-image computer vision," *Proceedings of Photogrammetric week*, pages 7–19. Institute for Photogrammetry, Stuttgart University, 1991.

[3] S. T. Barnard, "Stereo matching by hierarchical microcanonical annealing," Technical Report 14, SRI – International Technical Note., February 1986.

[4] H. Ebner and C. Heipke, "Integration of digital image matching and object surface reconstructure," *Proceedings of 16th ISPRS*, volume 27, pages 534–545. ISPRS, Comm.III.

[5] U. V. Helava, "Object space least squares correlation," *Proceedings of ISPRS*, volume 27B3, pages 321–331, Kyoto, 1988. ISPRS, Comm.III.

[6] M. Li. *Hierarchical Multi-point Matching with Simultaneous Detection and Location of Breaklines*. PhD thesis, Department of Photogrammetry, The Royal Institute of Technolgy, Stockholm, 1989.

[7] M. Li, "Hierarchical multipoint matching," *Photogrammetric Engineering and Remote Sensing*, (8):1039–1048, 1991.

[8] R. March, "Computation of stereo disparity using regularzation," *Pattern Recognition Letters*, 1988.

[9] U. A. Rauhala, "A revire of array algebra," *Proceedings of ISPRS*, Helsinki, 1976. Comm. III, International Society for Photogrammetry.

[10] U. A. Rauhala, "Array algebra as general base of fast transforms," *Comm. III Image Processing Symposium*, Graz, 1977. International Society for Photogrammetry.

[11] U. A. Rauhala, "Array estimation in signal processing," *Photogrammetric Engineering and Remote Sensing*, 48(9):1437–1444, 1982.

[12] U. A. Rauhala, "Compiler position of array algebra technology," *Proceedings of ISPRS, Comm.III Symposium*, volume 26, pages 173–198, Rovaniemi, Finland, 1986. ISPRS.

[13] U. A. Rauhala, "Compiler positioning system: An array algebra formulation of digital photogrammetry," *Photogrammetric Engineering and Remote Sensing*, (3), 1989.

[14] U. A. Rauhala, D. Davis, and K. Baker, "Automated dtm validation and progressive sampling algorithm of finite element array relaxation," *Photogrammetric Engineering and Remote Sensing*, (4), 1989.

[15] D. Rosenholm, "Accuracy improvement of digital matching for evaluation of digital terrain models," *Proceedings of ISPRS*, volume 26, pages 573–587, Rovaniemi, 1986. ISPRS, Comm.III.

[16] D. Rosenholm, "Multi-point matching using the least squares technique for evaluation of three-dimensional models," *Photogrammetric Engineering and Remote Sensing*, VIII(6), 1987.

[17] D. Rosenholm, "Multi-point matching along vertical lines in spot images," *International Journal of Remote Sensing*, 9(10), 1988.

[18] D. Terzopoulos, "Regularization of inverse visual problems involving discontinuity," *IEEE PAMI*, 8:413–424, 1986.

[19] M. Weisensee, "Modelle und algorithmen fur das facetten – stereosehen," Technical Report 374, Deutsche Geodatische Kommission, Munich, 1991.

[20] B. Wrobel, "Facets stereo vision (fast vision) – a new approach to computer vision and to digital photogrammetry," *Proceedings of Intercommission Conference of ISPRS on Fast Processing of Photogrammetric Data*, Interlaken, 1987. ISPRS.

[21] Y. Zhang. *Stochastic Stereo Matching with Neural Network*. PhD thesis, Zhenzhou Technical University of Surveying and Mapping, Zhenzhou, China, 1990. in chinese.

982

International Archives of Photogrammetry and Remote Sensing. Vol. XXXI, Part B3. Vienna 1996